Modelling texture perception by soft epithelial surfaces

George A. van Aken[ab]

Received 12th August 2009, Accepted 17th November 2009
First published as an Advance Article on the web 4th January 2010
DOI: 10.1039/b916708k

This paper introduces a mechanistic approach to relate the sensations of touch by epithelial surfaces of for example skin, eye or mouth to the material properties of the substrate. The approach is to model the hydrodynamic and frictional forces exerted by the substrate onto the surfaces, which are deformable and compliant to these forces. Subsequently these forces are related to the neurological responses of the mechanoreceptors buried in these surfaces. The potential of the approach is illustrated for textural perception of food materials in the mouth. It leads to several concepts for textural perception in the mouth, some of which have been demonstrated previously and some of which are new. As a first example, the branching into high and low viscosity regimes for thickness perception found experimentally can be linked directly to the detection limit of the neural receptors. As a second example, by taking into account the intrinsic roughness and deformability of the papilla surface, estimates are obtained for the cross-over between the hydrodynamic friction regime, where the papilla tips are lubricated by a thin liquid film (smooth mouthfeel), and the boundary friction regime, where the papilla tips are in direct contact with the opposing surface of the palate (rough mouthfeel). This has implications for the role of viscosity on smoothness and astringency sensations. As a final example, the model suggests that the sensation of hard particles (grittiness) can be suppressed by increasing the viscosity of the medium, which is in agreement with experimental findings from sensory studies.

Introduction

Human touch sensations are important for the assessment of the surface texture of materials. An example concerns the subjective evaluation of dry material surfaces such as textiles, wood, leather, coatings and plastic surface finishing by touch with skin (often the finger tip). Experimental studies have demonstrated an important role of both the surface roughness and friction forces in this evaluation.[1–5] Using a tribological probe microscope, Liu *et al.* demonstrated that the sensory ratings along the principal axes of rough–smooth and grippy–slippery are strongly correlated with measured surface roughness and the friction coefficient.[4] The other way round, frictional measurements have been used to assess skin condition and pathology[6–10] and the way skin condition can be improved by moisterizers, conditioners and creams.[10,11] Another example is contact lens comfort. The contact lens normally floats on a thin layer of tear fluid on the eye. It is thought that the discomfort experienced by the wearer is determined by friction forces generated by sliding motion of the contact lens surface and the corneal surface of the eye.[12,13] A final example is the sensation of food texture by the mouth. Various studies have demonstrated that the textural perception of food in the mouth is determined by a combination of the sensations of fracturing of solid material, rheological and frictional forces and the presence of particles in the mouth.[14–20]

Although various material parameters that relate to the sensation of touch can be measured instrumentally, the evaluation of their sensory effect is still highly dependent on the subjectivity of sensory panel scores.

This paper shows that this subjectivity can be overcome by clarifying the mechanisms that relate the mechanical forces induced by the structure and rheological and frictional properties of the material that is probed to the sensitivity and specificity of neural mechanoreceptors.

The approach is to model the forces exerted onto the receptors, taking into account the shape and deformability of the tissues that embed the receptors, and relate these forces to the specific sensitivity of the receptors involved. The potential of the approach will be demonstrated for the textural perception of food material in the mouth, focusing mainly on the roles of the

[a]TI Food and Nutrition, P.O. Box 557, 6700 AN Wageningen, The Netherlands
[b]NIZO Food Research, P.O. Box 20, 6710 BA Ede, The Netherlands

George A. van Aken

George van Aken graduated in physical chemistry and theoretical physics at the University of Utrecht, the Netherlands. In 1990 he defended his PhD thesis on microemulsions. He currently holds a position of senior scientist in food physics at NIZO food research, in which he works on various subjects related to food emulsions and fats. His main research topics are on fat crystallization, colloidal instabilities, hydrocolloids and emulsifiers. Within TI Food and Nutrition he explores the interactions of food material with the human body, such as the behavior of food emulsions in the mouth and gastro-intestinal tract.

force threshold of the mechanoreceptors in the tongue and the roughness and deformabilty of the papillae.

Aspects of mouthfeel

The perception of food texture in the mouth can be described by a range of sensory attributes such as *hard*, *thick*, *tough*, *brittle*, *sticky*, *rough*, *slimy*, *smooth*, *gritty*, *creamy*, *coating* and *astringent*. These textural sensory attributes are related to the behaviour of the food material in the mouth rather than the behaviour of the native food. At the time of perception, the food structure usually has changed considerably due to temperature changes, flow and the interaction with saliva and oral surfaces.[21] To give a few examples, gels are broken down to small fragments by mastication,[14,19,22] viscosity and firmness produced by starch largely disappears in the mouth because of starch hydrolysis by salivary amylase,[22,23] the viscosity of thin liquid emulsions increases on mixing with saliva,[24] and food material may be retained at the tongue surface, both in form of an adherent layer of food components such as proteins and starches at the tongue surface[25] and in the form of a thin coating of food material mixed with mucus and saliva.[26]

This section describes various aspects of tactile perception from different scientific disciplines, combining them into one picture of how mechanic properties of food materials might be interacting with the mechanoreceptors responsible for tactile perception.

Somatosensory perception

From a general neurological viewpoint, somatosensory perception in the mouth comprises a range of sensory modalities including touch, temperature perception, proprioception (detection of the position of the tongue and jaw) and nociception (involved in pain). The modality of touch corresponds to the detection of forces by neural mechanoreceptors. A distinction can be made between forces exerted on the hard surfaces of teeth and forces exerted on the soft epithelial surfaces that cover the mouth internally. The forces exerted on the teeth relate to sensory attributes such as *hard*, *tough* and *brittle*, which are relevant for solid foods. The forces exerted on the epithelial surfaces relate to the rheological and textural behaviour of food material that is in a fluidic state in the mouth. These correspond to sensory attributes such as *thick*, *slimy*, *sticky*, *rough*, *smooth*, *gritty*, *creamy*, *coating* and *astringent*.

Although a broad variety of tactile sensory attributes can be distinguished for fluidic materials, only a limited number of mechanoreceptor types exist, which will be discussed below in more detail. The broad range of tactile sensory attributes must therefore be derived by combination of the signals from these mechanoreceptors, the way they react on variables such as flow induced by gravity, direction and speed of the tongue movements and temporal variations such as relaxation and gradual loss of structure. Insight in the way stimuli are integrated in the brain into the various sensory attributes described by a sensory panels, and the role of learning and appreciation in this, is developed by Rolls *et al.*[27–29]

In a study of neural response of mechanoreptors at the tongue surface of healthy volunteers, Trulsson and Essick measured in one person the effect of touching the dorsal surface of the tongue with thin wires connected to force tranducers.[30] Mechanoreceptors in the tongue could be catagorized as superficial and deep receptor units, related to their depth underneath the surface. A total of 11 deep units were identified. These units are embedded in the muscle mass of the tongue and detect aspects of muscle tension. A total of 22 superficial receptor units were found. These units are located closely underneath the epithelial surface and are sensitive to touch. The superficial receptor units had receptive fields ranging between 1–19.6 mm^2, with an average of 2.4 mm^2, which is considerably larger than the typical dimensions of a single filiform papilla. The force threshold of these receptors ranged between 30–2000 μN, with an average of 150 μN. The superficial receptor units could be divided into slowly adapting (SA), rapidly adapting irregular (RA irregular) and rapidly adapting regular (RA regular) mechanoreceptors. Most abundant were the SA and RA regular receptors. The RA regular receptors, of which 14 were found, were especially sensitive to rapid force vibrations, which are probably relevant for sensory descriptors such as roughness and grittiness. These receptors had receptive fields ranging between 1–12.5 mm^2, with an average of 2.0 mm^2. The force threshold of these receptors ranged between 30–500 μN, with a geometrical mean of 110 μN. The SA regular receptors, of which 8 were found, were especially sensitive to maintained deformation of the mucosa, and for this reason are probably relevant for the perception of maintained local pressures or tangential forces. These receptors had receptive fields ranging between 1–19.6 mm^2, with a geometric mean of 3.3 mm^2. The force threshold of these receptors ranged between 60–2000 μN, with a geometrical mean of 270 μN.

From these observations it appears that the receptive fields of the superficial receptors are substantially larger than the typical dimensions of a single filiform papilla (as described below). Assuming that the forces that excite one neural afferent at different positions on its receptive field are additive and at this point neglecting the difference between RA and SA units, a lower force threshold of 30 μN/2.4 mm^2 corresponds to a lower stress threshold of about 12 Pa. Similarly, an average force threshold of 150 μN/2.4 mm^2 corresponds to an average stress threshold of about 60 Pa.

Rheology

Except for some special cases, such as the sparkling sensation caused by bubble nucleation and gas release from carbonized drinks, the forces that excite the mechanoreceptors are driven either by gravity or by the active motion of the tongue and jaws, and modified by the structural and flow properties of the food in the mouth.

Several authors have demonstrated for Newtonian fluids that the sensory attribute *thick* is highly correlated to the instrumental viscosity as measured outside the mouth. Because many food products are shear thinning, much attention has been given to determine the governing shear rate in the mouth. A high correlation is often found for moderate shear rates of around 50 s^{-1}, although a slightly better correlation was found with the complex viscosity at 50 Hz if weakly gelling solutions of xanthan were included.[31] By sensory panelling of various food products Shama and Sherman identified windows of instrumental shear stresses

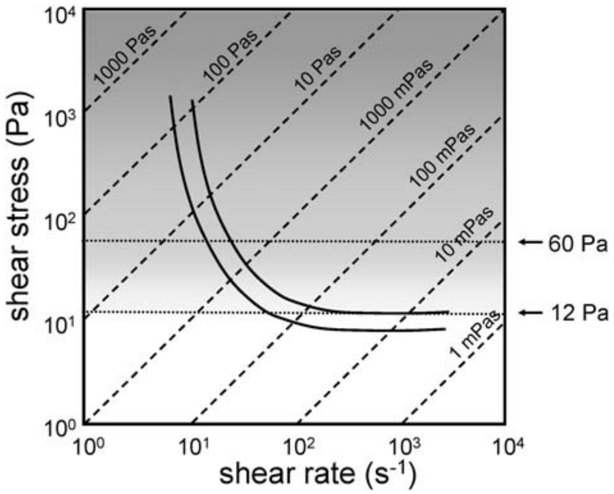

Fig. 1 Range of instrumental shear stress *versus* shear rate windows that correspond to the rheological regimes applied in the mouth during thickness rating. Redrawn after: Shama, F. and P. Sherman (1973). The gray-scale indicates the expected excitation of the superficial mechanoreceptors in the tongue, with lower and averaged stress thresholds of 12 and 60 Pa, respectively.

and shear rates corresponding to products with similar thickness ratings but different shear-thinning behaviour.[32] These windows correspond to the rheological regimes applied in the mouth during thickness rating. The governing shear rate was shown to be dependent on the viscosity of the product itself. The experimental windows group into two main branches (Fig. 1), which were confirmed by an additional study on viscosity scoring of glucose syrups by distance and ratio scaling procedures.[33] At high shear rate (>100 s^{-1}) the shear stress is low, about 10 Pa, and the corresponding viscosities are typically lower than 100 mPa·s. For liquids with a viscosity above 1 Pa·s, the shear rates are typically between 10 and 50 s^{-1}. The concept of Shama and Sherman has been refined by Cutler and coauthors[34] and Morris,[35] extending it to the shear thinning behavior of polysaccharide solutions with viscosities corresponding to the high-viscosity branch. These newer studies confirmed that the perceived thickness of a shear-thinning polysaccharide solution with higher viscosity is related to the viscosity at a shear rate of about 10 s^{-1}, which is thought to be representative for oral processing. An improvement was obtained by including the change in viscosity with shear rate ($d\eta/d\dot{\gamma}$) at 10 s^{-1}.

Adopting the concept of Shama and Sherman[32] (and focusing on Newtonian liquids), comparison can be made between the magnitude of the shear stresses involved in thickness perception according to Fig. 1 and the range of stresses that can be sensed by the mechanoreceptors according to the neurological measurements by Trullson and Essick.[30] This is illustrated in Fig. 1, where the minimum and averaged threshold stresses for the RA mechanoreceptors are shown in the plot by Shama and Sherman. Interestingly, the minimum threshold for sensation by the RA mechanoreceptors is above the shear stress in the high shear rate (low viscosity) branch, while the cross over between the low and high viscosity branches corresponds roughly to the averaged stress threshold of the RA mechanoreceptors. This agrees with the explanation put forward by Shama and Sherman that the perception of viscosity of thicker liquids relates to viscous forces at the tongue surface (caused by shear flow induced by tongue movements), while the perception of viscosity of thinner liquids is more related to the speed by which a liquid spontaneously flows (for example by gravity) through the mouth.

Tribology

It has been recognized that, in addition to the rheological behaviour, also the frictional behaviour of the tongue surface is important for tactile sensory perception. For example, important for many food products is the desired attribute *creamy*, which is thought to be composed of both viscosity and frictional textural stimuli,[15] besides flavour contributions. Frictional properties are commonly measured using a tribometer, which measures the traction force between two bodies in rubbing motion.

As a measuring instrument, the mouth resembles a tribometer rather than a rheometer. In a rheometer, the geometry and the relative positioning of the measuring surfaces are fixed. For example, in a Couette cell the gap between the inner and outer cylinders is fixed at a finite distance of typically 1 mm. In contrast, in a tribometer the gap between the two measuring surfaces is variable, determined by the sum of the constant normal force by which the two surfaces are pushed together and the lift force generated by the material between the surfaces. Two principally different tribological regimes can occur between two sliding surfaces. In the hydrodynamic regime, the liquid is hydrodynamically forced between the two opposing surfaces, generating a lift force that is sufficiently large to compensate the normal force pushing the surfaces together, in this way keeping the surfaces separated. The friction force in the hydrodynamic regime is determined by the rheological properties of the liquid. In the boundary regime, on the other hand, the hydrodynamic lift force is too small to compensate the normal force at any separation, and therefore two surfaces are in sliding contact. In this case the friction force is determined by the surface properties (*e.g.* hydrophobicity, surface roughness and adhesion of surface actives).[36–38]

Tongue histology

Returning to the perception of viscous and drag forces by the tongue surface, the mechanoreceptors involved are embedded within the papillae, which roughen the dorsal side of the tongue. The most abundant type of papillae, the filiform papillae, are innervated by tactile sensors. Any force transferred to the mechanoreceptors must therefore be related to a deformation of the filiform papillae, which in principle can be described by the visco-elastic deformation properties of these papillae.

The structure of the filiform papillae is complex (Fig. 2). In mammals, each filiform papilla consists of a primary papilla of connective tissue, structured at the dorsal surface by secondary papillae of connective tissue. By cell growth at the surface of these secondary papillae, a layer of stratified squamous epithelium is formed, in which the outermost cells loose the nucleus and organelles and become flattened parallel to the surface and have a fine fibrillar cytoplasm. In this way a scale is formed at the dorsal surface. Because of the shape of the secondary papillae, this scale has a tube-like structure. In most mammal species, the tube surface is hardened by keratinisation of the cells, forming

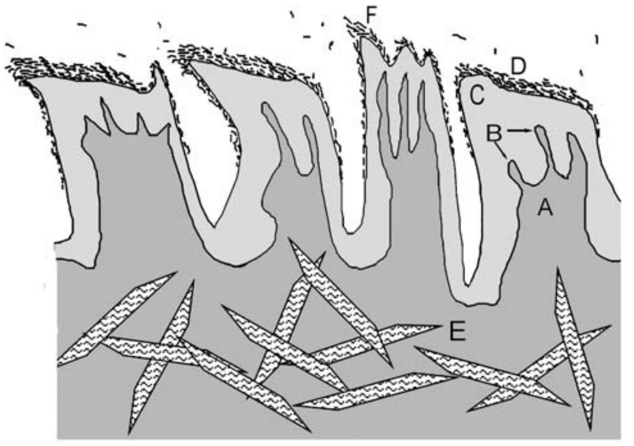

Fig. 2 Sketch of filiform papillae (based on various literature sources). Shown are 4 papillae on the dorsal side of the tongue, with the tongue tip at the right side. A: primary papilla of connective tissue; B: secondary papillae; C: stratified squamous epithelium; D: layer of desquamizing partially keratinized surface cells; E: muscle fibres; F: epithelial thread. Typical averaged width of a filiform papilla is 250 μm, which varies between individuals.

threads extending from the papilla tips. These structures resist wear, give the tongue surface a certain grip to the food material or even serve as a rasp. In humans, however, keratinisation of the epithelial surface is incomplete or almost absent,[39] although fully keratinised epithelial threads are sometimes found at the rim of the tubes. Instead, groups of almost undifferentiated basal cells are present, which are thought to compensate for the increased wear of the incompletely keratinised cells by accelerated regeneration. As a consequence, the surface of human filiform papillae show a high rate of desquamation, forming a surface plaque with variable thickness and containing desquamized surface cells, bacteria and mucous material.

The complex structure of the papillae makes it difficult to accurately model their deformation. For the present purpose it suffices to use a highly simplified model, describing the papillae as smooth elastically deformable bodies. The elasticity modulus is estimated from *ex vivo* measurements of the elasticity modulus of cylindrical plugs cut out of fresh piglet tongue by Dresselhuis *et al.*[40] The measured value varied between approximately 0.7 and 3 kPa, dependent on the location at the tongue surface and the thickness of the cylindrical sample. An averaged value for the central part of the tongue is 2.6 kPa. The actual value of the elasticity modulus of the papillae *in vivo* might be somewhat lower, because the cylindrical plugs also contain muscular tissues buried deeply below the tongue surface, and these tissues harden because of rigor mortis. The low measured values suggests that the papilla body is very soft and deformable. It is expected that the rough desquamising layer of partially keratinised cells at the surface of the papillae will be harder than the tissues of the papilla body underneath. This layer is taken into account by assuming a surface roughness on the order of 20 μm, which corresponds to the typical size of the desquamizing cells. This is about 10% of the papilla diameter, which seems to be a reasonable estimate on the basis of various microscopic images of cross sections of the papillae.

Tribological modelling

A soft tribological model is used to estimate the hydrodynamic lift force and friction experienced by a single papilla when it is rubbed against the palate. For this, a theory for fluid-induced lubrication of soft interfaces in the hydrodynamic flow regime described by Skotheim and Mahandevan[41] was adopted. A detailed description of the theory is given in the appendix. To apply the theory the palate surface is approximated as a hard flat surface and the papilla as a blunt-shaped homogeneous elastic body protruding from a hard undeformable surface (Fig. 3).

As a first approximation, it is assumed that the papilla at rest is symmetrical ($\alpha = 0$) in the direction of motion, with a shape described by x^n, where x is the distance along the direction of motion and $n = 4$. The hydrodynamic calculations are carried out in two dimensions, which actually corresponds to modelling the 3-dimensional papilla as an infinitely long ramp perpendicular to the direction of flow. The shape of the deformed papilla is determined by the dimensionless deformation parameter η, given by

$$\eta = \frac{l\mu U}{h_0^3}\frac{\Delta h}{p} \tag{1}$$

where μ is the viscosity of the fluid between the opposing surfaces, h_0 is the distance between the surfaces at $x = 0$, and p is the local gap pressure. For $\eta = 0$ the papilla is undeformed, and deformation increases for larger values of η. The papilla is furthermore assumed to be elastic and deformation is described according to Hooke's law,

$$\frac{\Delta h}{He} = \frac{p}{E_p} \tag{2}$$

where He is the vertical height of the papilla and E_p is the Young's modulus of the papilla. For the model calculations, the following estimates were made for the model parameters: dimensions of the filiform papilla $l \approx 250$ μm and $He \approx l$, the typical speed of the tongue $U = 1$ cm s^{-1}, and papilla modulus $E_p = 2.6$ kPa.

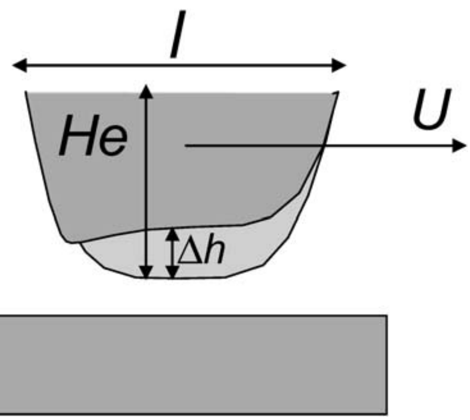

Fig. 3 Definition of model parameters used to describe the deformation of a papilla: l, He and U are the length, height and velocity of the papilla, respectively. The vertical deformation is given by Δh. For convenience, the tribo-pair is depicted upside down. The modelled shape of the papilla corresponds to $n = 4$, and $\mu = 0$ (light grey) and 15 (dark grey), respectively (parameters explained in the appendix). Note that the papilla is depicted in the upside-down position, conforming to the convention in tribological literature.

To proceed from this point, assumptions must be made on the normal forces applied on the tongue surface. The difficulty is that these normal forces are obviously highly variable, dependent on the force by which the tongue is pushed against the palate. This force will depend on the material that is present in the mouth, through a neurological feedback mechanism. The sensory results of Fig. 1 suggest roughly defined regimes of shear stress and shear flow operational for thickness perception. A best fit through the experimental regions of instrumental shear stress (τ, expressed in Pa) and experimental shear rates ($\dot{\gamma}$, expressed in s^{-1}) that best correlate with thickness perception over a range of food products with varying shear thinning behaviour yields

$$\tau = 1000 \cdot (\dot{\gamma} - 8)^{-1.3} + 10 \quad (3)$$

while the viscosity is determined by

$$\mu = \frac{\tau}{\dot{\gamma}} \quad (4)$$

If the hydrodynamic friction forces f_f per unit area at the papilla surface are set equal to the shear stresses τ involved in the perception of thickness according to eqn (3), calculations yield values for the minimum gap width relevant for the conditions during thickness perception. The results are listed in Table 1. This table shows that the calculated minimum gap width for the deformed soft surface is always roughly a factor 2 larger than the hydrodynamic gap width of the papilla calculated by dividing the speed of papilla motion by the shear rate. The reason for this is that for the soft papilla tip the shear force also contains a contribution from the pressure difference between the entry and exit of the gap, which is related to the wig-shaped deformation of the papilla surface. The calculated lift pressure decreases quickly with the viscosity, and already becomes smaller than the shear stress at a viscosity somewhat larger than 10 mPa·s. At the same time, the calculated minimum gap width becomes larger than the surface roughness of the papilla only for viscosities larger than 10 mPa·s.

Below 10 mPa·s, even at the very high shear rates suggested by Fig. 1, the gap width obtained by the hydrodynamic lift remains too small to overcome the surface roughness of the papilla surfaces. As a consequence, in this regime the main forces exerted onto the papilla surfaces by rubbing tongue against palate will not be hydrodynamic in origin, but result from boundary friction of surface asperities.

At higher viscosities, the calculated gap width quickly increases to values much larger than the surface roughness. In fact it is seen to rise to values much larger than the height of the papilla, which would be beyond the approximations made in the model. However, now the calculated lift pressure becomes unrealistically small. In reality, the tongue muscle will easily produce normal stresses that are many orders of magnitude larger than the calculated lift pressures. To investigate the effect of such a deliberately applied normal force, the calculations were repeated for the situation where a normal pressure of 100 Pa compensates the lift pressure. From Table 2 it can be seen that if the lift pressure is set at this value of 100 Pa, the minimum gap width is smaller than the surface roughness of the papilla for viscosities below 20 mPa·s, and the shear stresses exceed the normal pressures for viscosities larger than approximately 250 mPa·s (as found by interpolation). Increasing the normal pressure decreases the gap width.

As described in the section on tongue histology, the Young modulus of the tongue varies somewhat. The importance of this variability on the model calculations is illustrated in Table 3. As can be seen, the minimum gap width does not vary within the accuracy of the model calculation. The lift pressure increases with E_p, but for the measured variation in the Young modulus (0.7–3 kPa), the resulting variation in the lift pressure is within a factor 4, and remains much smaller than the variation caused by the viscosity changes demonstrated in Table 1.

One may wonder how long it takes to reach the steady-state of lubrication (either in the boundary or hydrodynamic lubrication regime) described above in relation to Table 1 and Table 2. An estimate of this time can be obtained from the well known Reynolds model for the rate of thinning of a liquid film with

Table 1 Results of lift pressures and minimum gap width calculated from the tribological model, assuming $n = 4$ for the shape of the undeformed papilla and conditions corresponding to thickness perception, as described by eqn (3)

Viscosity, μ (mPa·s)	Typical shear rate for thickness perception, $\dot{\gamma}$ (s^{-1})	Typical shear stress for thickness perception, τ (Pa)	Calculated lift pressure, p (Pa)	Calculated minimum gap width (μm)	Deformation parameter, η	Hydrodynamic gap width at $U = 1$ cm s^{-1}, calculated as $d = U/\gamma^{\cdot}$ (μm)
4	2510	10.04	73.18	9.35	3.33	4.00
10	1013	10.13	11.09	21.4	0.243	9.87
100	121.3	12.13	0.029	183	0.00395	82.6
1000	29.05	29.05	0.00232	763	0.000543	345
10 000	13.08	130.8	0.00429	1693	0.000495	765

Table 2 Results of lift pressures and minimum gap width calculated from the tribological model, assuming $n = 4$ for the shape of the undeformed papilla, for a tongue pressure of 100 Pa, and a tongue velocity $U = 1$ cm s^{-1}

Viscosity, μ (mPa·s)	Shear rate, $\dot{\gamma}$ (s^{-1})	Shear stress, τ (Pa)	Lift pressure, p (Pa)	Calculated minimum gap width (μm)	Deformation parameter, η
4	2836	11.345	100	8.789	7.465
10	1852	18.523	100	12.66	3.382
100	668	66.8	100	32.75	0.9128
1000	254	253.6	100	85.09	0.40943
10 000	99	990.3	100	218.9	0.22572

Table 3 Effect of variation in E_p on the model calculations, assuming $n = 4$ for the shape of the undeformed papilla and conditions corresponding to thickness perception, as described by eqn (3), for a viscosity of 10 mPa·s and shear rates and shear stresses typical for thickness perception (eqn (3))

Young's modulus of the papilla, E_p (kPa)	Calculated lift pressure, p (Pa)	Calculated minimum gap width (μm)	Deformation parameter, η
0.5	28.74	22.67	2.467
1	21.95	21.49	0.7950
5	6.086	21.57	0.1215
20	1.553	21.80	0.02993

Table 4 Calculated thinning time to reach the surface roughness of papillae, under conditions corresponding to the high-viscosity branch in Fig. 1. Further explanation in the text

Viscosity, μ (mPa·s)	Typical shear stress for thickness perception, τ (Pa)	Time to reach $h_t = 20$ μm (s)
4	10.038	0.0029
10	10.125	0.0072
100	12.134	0.060
1000	29.048	0.25
10000	130.82	0.56

viscosity μ between two plane parallel plates of radius R and at distance h, pushed together by pressure p:

$$-\frac{dh}{dt} = \frac{8h^3 p}{3\mu R^2} \tag{5}$$

neglecting inertia effects and the contribution of the surface tension of the liquid. Subsequent integration yields

$$h_t = \frac{1}{\sqrt{\frac{16pt}{3\pi\mu R^2} + \frac{1}{h_i^2}}} \tag{6}$$

where h_i is the initial distance between the plates, and h_t is the distance at time t after the pressure is applied. Setting $R = ½l \approx$ 125 μm as the typical radius of a papilla tip, making the approximation $h_i = \infty$, and estimating that under these conditions the normal stresses would be of similar magnitude as the frictional stresses taken from Fig. 1 or eqn (3), leads to thinning times given in Table 4.

The table shows that for viscosities up to about 100 mPa·s, the time needed for thinning until boundary lubrication is achieved is probably too short to be noticed. For higher viscosities this thinning may take sufficient time to be sensed. The delay in achieving boundary lubrication might be a sensorial measure for high viscosity.

Discussion

First a remark about the limitation of using a 2-dimensional model. In general, for a 2-dimensional model the calculated gap width will be an overestimation for the actual 3-dimensional case. This is because in the 3-dimesional case, liquid can flow out sideways from the gap, reducing the gap pressure. Despite this limitation of a 2-dimensional papilla, a number of trends are suggested by the model calculations.

For thin liquids (viscosities below approximately 100 mPa·s, corresponding to the horizontal regime in Fig. 1), hydrodynamic friction forces are too small to be detected by the mechanoreceptors. Even for very small normal pressures, the gap between tongue papillae and palate produced by the hydrodynamic lift forces becomes smaller than the surface asperities of the papilla tips. Therefore, any attempt to increase the hydrodynamic shear force by increasing the normal pressure results in boundary friction forces. In this regime, the shear stresses related to viscosity of the liquid can therefore not be sensed by the mechanoreceptors. It is likely that the condition of boundary friction of the papilla tips is picked up as a high frequency vibration by the fast-responding mechanoreceptors. This may explain the notion of "raw tongue" or "sandpaper tongue" as a typical description by a sensory panel for these liquids. In this regime, the sensation of viscosity is likely related to other physical phenomena, such as the speed by which the liquid spontaneously spreads through the mouth by gravity.

Liquids which fall in the regime of viscosities well above the bend in Fig. 1, corresponding to "effective" viscosities well above 1000 mPa·s, are for example condensed milk, syrups or paste-like textures. The time needed to thin the liquid layer until contact between papilla and palate is achieved by pushing the tongue against the palate, becomes considerable and is likely sensed as a measure of viscosity. Furthermore, in a rubbing motion of the tongue against the palate, the hydrodynamic friction stress will easily dominate the applied normal pressure, and the friction stresses will be large enough to be picked up as a constant force by the slowly adapting mechanoreceptors. Indeed, liquids with viscosities in this regime are often described as "thick" (suggesting viscous forces) if the material does not slip on the tongue surface or "slippery" if the material slips on the tongue surface (suggesting negligible boundary friction).

In the transition between these two main regimes in Fig. 1, the friction will be a mix of hydrodynamic friction forces and boundary friction forces, and likely more textural information can be obtained by deliberate variation of the applied normal pressure.

An aspect that should be taken into account at this point is the presence of saliva in the oral cavity. Saliva is a shear-thinning fluid for which a viscosity typically around 2 mPa·s at relevant shear rates is reported by various authors.[42] By the action of mucins, saliva acts as a (boundary) lubricant for the tongue surfaces[38] and can induce flocculation of emulsion droplets,[24,43,44] and contains amylase, which hydrolyses starch.[23,45] For high-viscosity systems, the gap width will remain relatively large, unless a high pressure is deliberately applied. The viscosity is then probed as an average over the gap width, and since it will take some time before the food material is mixed with saliva, the viscosity probed in the mouth will be closely related to the rheological properties of that food material before it has been taken into the mouth. For low viscosity systems, however, the gap will rapidly decrease to small widths, which during rubbing motion of the tongue will lead to efficient mixing of the food material with saliva and an intense contact with the tongue and palate surfaces. This will cause drastic changes structural and rheological properties of the food material; the perceived viscosity and lubrication behaviour can strongly deviate from the expectation based on the rheological behaviour of the food material before intake.

For example, because of the breakdown of starch by salivary amylase, any starch-thickened food system is judged as much thinner than expected on the basis of the viscosity before intake.[23,45] As another example, for emulsions, saliva-induced droplet aggregation close to the top of the tongue surface probably increases the perceived viscosity compared to the viscosity before intake. It has been shown that if a liquid emulsion is mixed with saliva at a 1 : 1 ratio, the viscosity may easily increase by a factor 5.[24] The increased viscosity might promote hydrodynamic lubrication, giving the sensation of a better lubricated "smoother" tongue and a more viscous tongue "coating". Furthermore, emulsions can deposit oil onto the papilla surfaces.[46,47] This was shown to lead to a reduction in boundary friction, which may also relate to the sensation of a smoother tongue. Indeed, the perception of smoothness and a tongue coating seem to contribute to the perception of creaminess of food emulsions.[21,48] Based on the concepts derived in this paper, the sensation of a smoother tongue resulting from a reduced boundary friction (for example by deposition of oil), or a raw tongue resulting from an increased boundary friction (for example because the natural lubricaticity of the mucous layer is attenuated by low pH or astringent agents), can only be relevant for viscosities below approximately 100 mPa·s in the mouth (corresponding to the horizontal regime in Fig. 1). For high viscosity food materials the effect of boundary friction on perception can however only be relevant after the viscosity is sufficiently reduced in the mouth, for example by disruption of a gelled matrix, breakdown of starch by salivary amylase and dilution with saliva, and for this reason will be more relevant for after-feel sensations.

Some prediction can also be made on the effect of hard particles present in the food material. Obviously, if the particle size exceeds the minimum gap width between the papilla tip and the palate, pushing particles through this gap would give rise to another rapidly varying force at the papilla surface, which would be picked up by the rapidly adapting mechanoreceptors and be recognized as "gritty". This condition will be reached sooner (at lower normal pressure of the tongue) if the viscosity of the suspending liquid is lower. This is indeed observed experimentally.[20]

Conclusion

By describing the forces exerted onto the soft epithelial surfaces of tongue papillae on the basis of a tribological model and comparing these forces with the sensitivity of the neural mechanoreceptors that are responsible for perception, some interesting conclusions can be drawn.

The model calculations suggest that the viscosity in the mouth can only be judged from the direct sensation of hydrodynamic friction forces induced by tongue movement and the time needed to thin the fluid layer between tongue and palate if the viscosity of the product is quite high, for example more than 1 Pa·s. For food materials with a lower viscosity, the forces on the tongue and palate surfaces are increasingly dominated by boundary friction between these surfaces, which is affected by the presence of adsorbed material such as salivary protein, emulsion droplets, fat, lipids and surfactants. The sensation of boundary friction is likely related to sensory descriptors that are not directly related to the viscosity, such as roughness, dryness and astringency. For viscosities below approximately 100 mPa·s, therefore, the viscosity can only be distinguished by other aspects, such as the speed by which the fluid distributes through the mouth or the time needed to thin the liquid film between tongue and palate to such a value that boundary friction is sensed.

The approach of rheological and tribological modelling of the forces exerted onto the receptors and relating these forces to the specific sensitivity of the receptors involved, gives objective thresholds for the sensation of material parameters (*e.g.* roughness, particle size, viscosity, time of spreading). It excludes certain mechanisms (*e.g.* the direct sensation of viscous forces for low viscosity liquids) and suggests other mechanisms (*e.g.* time of spontaneous spreading in the mouth and boundary friction sensations for low viscosity liquids). In the hydrodynamic model calculations, the only physical parameter that has so far been introduced is the viscosity. It would be interesting to introduce rheological parameters related to the viscoelasticity of food materials (*e.g.* shear thinning viscosity, elongational viscosity, normal forces) explicitly in the hydrodynamic equations. The approach can furthermore be extended by also including the response (firing rate as a function of force) of the mechanoreceptors. It is expected that a similar approach for other epithelial surfaces, such as those of skin and eye, can also enhance the mechanical understanding of textural perception by these surfaces.

Soft lubrication model

Skotheim and Mahandevan[41] described fluid-induced lubrication of soft interfaces in the hydrodynamic flow regime in two dimensions. In this regime, the flow of liquid between the two surfaces produces a lift force that exceeds the normal force pushing the surfaces together. Because of this, the surfaces remain completely separated. Based on the Navier–Stokes equation, the lift-force of a 2-dimensional deformable rim moving along a deformable surface was calculated.

Starting point is the Navier–Stokes equations,

$$\begin{aligned} &\rho(\partial_t\vec{v} + \vec{v}\cdot\nabla\vec{v}) = \mu\nabla^2\vec{v} - \nabla p \\ &\nabla\cdot\vec{v} = 0 \end{aligned} \tag{A1}$$

where ρ is the density of the fluid and $\vec{v}$ is a vector representing the fluid velocity.

It is recognized that the gap width between two sliding surfaces in the hydrodynamic lubrication regime is usually sufficiently small that the flow can be considered laminar ($Re \ll 1$). If the flow can also be considered stationary, the Navier–Stokes equations reduce to

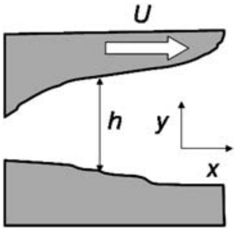

Fig. 4 Parameter definition and configuration of the gap between the two surfaces in tribological contact.

$$\begin{aligned} \mu\nabla^2\vec{v} &= \nabla p \\ \nabla\cdot\vec{v} &= 0 \end{aligned} \tag{A2}$$

These equations can be solved for each cross section across the gap (Fig. 4), yielding the expression

$$v_x = \frac{1}{2\mu}\frac{dp}{dx}\big(y(h-y)\big) + \frac{Uy}{h} \tag{A3}$$

However, the net flow through each cross section must be equal along the gap in the x-direction, requiring that Q must be independent of x, Q given by

$$Q = \int_0^h v_x dy \tag{A4}$$

This yields

$$\frac{dQ}{dx} = 0 = \frac{d}{dx}\left(6\mu U - h^3\frac{dp}{dx}\right) \tag{A5}$$

This differential equation was solved numerically, with the boundary condition of equal pressures at the entry and exit of the gap.

Once the pressure distribution along the gap is known, the hydrodynamic lift force can be calculated from

$$f_n = \int_l p dx \tag{A6}$$

and the hydrodynamic friction force from

$$f_f = \mu \int_l (\partial_z v_x)_{z\,=\,\text{surface}} dx \tag{A7}$$

The friction coefficient can be calculated from

$$c = \frac{f_f}{f_n} \tag{A8}$$

The overall blunt shape of a human filiform papilla is described by the expression,

$$h = h_0\left(1 + \alpha\frac{x}{l} + \frac{x^n}{l^n} + \frac{\Delta h\big(p(x)\big)}{h_0}\right) \tag{A9}$$

Here, h is the gap width at any position x, h_0 is the gap width between the undeformed papilla at $x = 0$ and the palate, l is the length of the papilla and Δh corresponds to the vertical deformation of the papilla caused by the local gap pressure $p(x)$

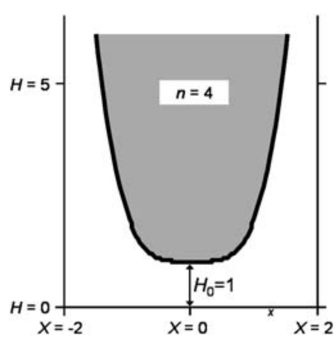

Fig. 5 Model of a papilla in scaled units, given by $n = 4$ and $\alpha = 0$. Scaled gap width $H = h/h_0$; scaled distance along the gap $X = x/l$.

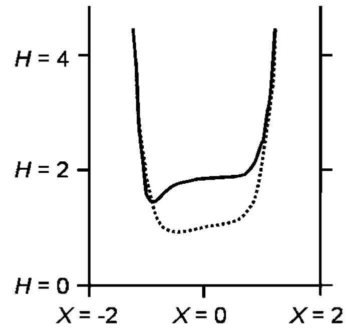

Fig. 6 Example of model calculations for $n = 8$, $\alpha = 1$ and $\eta = 5$: scaled gap width. Dotted line represents the undeformed papilla; drawn line represents the deformed papilla. Scaled gap width: $H = h/h_0$; scaled distance along the gap: $X = x/l$.

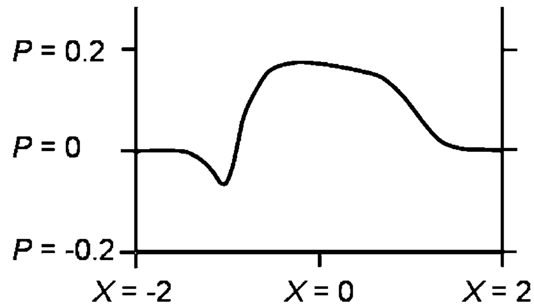

Fig. 7 Example of model calculations for $n = 8$, $\alpha = 1$ and $\eta = 5$. Scaled gap pressure: $P = \frac{h_0^2}{l\mu V}p$; scaled distance along the gap: $X = x/l$.

(Fig. 5). In eqn (A9), the parameter α describes the skewness of the gap, and n describes the overall shape of the papilla. A parabolic cross section corresponds to $n = 2$ and ($\alpha = 0$), whereas the actual overall shape of a papilla is much more flattened ($n > 2$) and slightly skewed ($\alpha \neq 0$).

The pressure-induced deformation of the papilla is described by the dimensionless softness parameter

$$\eta = \frac{l\mu V}{h_0^3}\frac{\Delta h}{p} \tag{A10}$$

An illustration of model calculations is given in Fig. 6 and Fig. 7. For the given case with $n = 8$, $\alpha = 1$ and $\eta = 5$ the friction coefficient is given by

$$c = 5.14\frac{h_0}{l} \tag{A11}$$

References

1 M. Zhang and A. F. T. Mak, *Prosthetics and Orthotics International*, 1999, **23**, 135–141.
2 M. Tanaka, S. Chonan, Z. Jiang and H. Nakajima, *Trans. Japan Soc. Mech, Eng. C*, 1999, **65**, 970–976.
3 X. Liu, M. K. Chan, B. Hennessey, T. Rübenach and G. Alay, *J. Phys. Conf. Ser.*, 2005, **13**, 357–361.
4 X. Liu, Z. Yue, Z. Cai, D. G. Chetwynd and S. T. Smith, *Meas. Sci. Technol.*, 2008, **19**, 084007–084016.
5 S. Derler, U. Schrade and L.-C. Gerhardt, *Wear*, 2007, **263**, 1112–1116.
6 J. S. Comaish and E. Bottoms, *Br. J. Dermatol.*, 1971, **84**, 37–43.
7 M. Lodèn, H. Olsson, T. Axell and Y. Werner, *Br. J. Dermatol.*, 1992, **126**, 137–141.

8 M. Lodèn, *Acta Dermato-Venerelog. (Suppl)*, 1995, **192**, 3–48.
9 M. Tanaka, *J. Mater. Process. Technol.*, 2001, **108**, 253–256.
10 N. Gitis and R. Sivamani, *Tribol. Trans.*, 2004, **47**, 461–9.
11 R. K. Sivamani, J. Goodman, N. V. Gitis and H. I. Maibach, *Skin Res. Technol.*, 2003, **9**, 235–239.
12 J. A. Nairn and T. Jiang, *Proc. ANTEC '95*, Boston, MA, May 7–11, 1995, 1995, 1–5.
13 A. C. Rennie, P. L. Dickrell and W. G. Sawyer, *Tribol. Lett.*, 2005, **18**, 499–504.
14 J. B. Hutchings and P. J. Lillford, *J. Texture Stud.*, 1988, **19**, 103–115.
15 J. L. Kokini, *J. Food Eng.*, 1987, **6**, 51–81.
16 G. Sala, PhD Thesis, Wageningen University, Wageningen, The Netherlands, 2007.
17 R. A. De Wijk and J. F. Prinz, *Food Qual. Preference*, 2005, **16**, 121–129.
18 R. A. De Wijk and J. F. Prinz, *J. Texture Stud.*, 2006, **37**, 413–427.
19 L. van den Berg, T. van Vliet, E. van der Linden, M. A. J. S. van Boekel and F. van de Velde, *Food Hydrocolloids*, 2007, **21**, 961–976.
20 L. Engelen, R. A. de Wijk, A. Van der Bilt, J. F. Prinz, A. M. Janssen and F. Bosman, *Physiol. Behav.*, 2005, **86**, 111–117.
21 G. A. Van Aken, M. H. Vingerhoeds and E. H. A. De Hoog, *Curr. Opin. Colloid Interface Sci.*, 2007, **12**, 251–262.
22 A. M. Janssen, M. E. J. Terpstra, R. A. De Wijk and J. F. Prinz, *J. Texture Stud.*, 2007, **38**, 42–69.
23 R. A. De Wijk, J. F. Prinz, L. Engelen and H. Weenen, *Physiol. Behav.*, 2004, **83**, 81–91.
24 M. H. Vingerhoeds, E. Silletti, J. De Groot, R. Schipper and G. A. van Aken, *Food Hydrocolloids*, 2009, **23**, 773–785.
25 H. H. J. De Jongh and A. M. Janssen, *J. Texture Stud.*, 2007, **38**, 70–86.
26 R. A. De Wijk, M. E. J. Terpstra, A. M. Janssen and J. F. Prinz, *Trends Food Sci. Technol.*, 2006, **17**, 412–422.
27 E. T. Rolls, J. V. Verhagen and M. Kadohisa, *J. Neurophysiol.*, 2003, **90**, 3711–3724.
28 E. T. Rolls, *Nutr. Rev.*, 2004, **62**, S193–S204.
29 E. T. Rolls, *Physiol. Behav.*, 2005, **85**, 45–56.
30 M. Trulsson and G. K. Essick, *J. Neurophys.*, 1997, **77**, 737–748.
31 E. R. Morris, in *Food Polysaccharides and their Applications*, ed. A. M. Stephen, Marcel Dekker, Inc., New York, 1995, pp. 517–546.
32 F. Shama and P. Sherman, *J. Texture Stud.*, 1973, **4**, 111–118.
33 F. Shama and P. Sherman, *J. Texture Stud.*, 1973, **4**, 254–262.
34 A. N. Cutler, E. R. Morris and L. J. Taylor, *J. Texture Stud.*, 1983, **14**, 377–395.
35 E. R. Morris, in *Food polysaccharides and their applications*, ed. A. M. Stephen, Marcel Dekker, Inc., New York, 1995, pp. 517–546.
36 J. H. H. Bongaerts, K. Fourtouni and J. R. Stokes, *Tribol. Int.*, 2007, **40**, 1531–1542.
37 J. H. H. Bongaerts, D. Rossetti and J. R. Stokes, *Tribol. Lett.*, 2007, **27**, 277–287.
38 G. E. Yakubov, J. McColl, J. H. H. Bongaerts and J. J. Ramsden, *Langmuir*, 2009, **25**, 2313–2321.
39 A. Plackova and M. Skach, *Z. Mikrosk. Anat. Forsch.*, 1975, **89**, 305–318.
40 D. M. Dresselhuis, E. H. A. De Hoog, M. A. Cohen Stuart and G. A. Van Aken, *Food Hydrocolloids*, 2008, **22**, 323–335.
41 J. M. Skotheim and L. Mahadevan, *Phys. Rev. Lett.*, 2004, **92**, 245509.
42 R. G. Schipper, E. Silletti and M. H. Vingerhoeds, *Arch. Oral Biol.*, 2007, **52**, 1114–1135.
43 E. Silletti, M. H. Vingerhoeds, W. Norde and G. A. Van Aken, *Food Hydrocolloids*, 2007, **21**, 596–606.
44 E. Silletti, M. H. Vingerhoeds, W. Norde and G. A. Van Aken, *J. Colloid Interface Sci.*, 2007, **313**, 485–493.
45 L. Engelen, R. A. De Wijk, J. F. Prinz, A. M. Janssen, A. Van der Bilt, H. Weenen and F. Bosman, *Physiol. Behav.*, 2003, **78**, 805–811.
46 D. M. Dresselhuis, H. J. Klok, M. A. Cohen Stuart, R. J. de Vries and V.A.G.A., *Food Biophys.*, 2007, **2**, 158–171.
47 D. M. Dresselhuis, M. A. Cohen Stuart, G. A. Van Aken, R. G. Schipper and E. H. A. de Hoog, *J. Colloid Interface Sci.*, 2008, **321**, 21–29.
48 G. A. Van Aken, M. H. Vingerhoeds and E. H. A. de Hoog, in *Designing functional foods*, ed. D. J. McClements, Woodhead Publishing Ltd., Cambridge, UK, ch. 19, pp. 481–501.

